Materials Science in Semiconductor Processing 16 (2013) 992–996

Contents lists available at SciVerse ScienceDirect

Materials Science in Semiconductor Processing

journal homepage: www.elsevier.com/locate/mssp

Defect studies in $Cu_2ZnSnSe_4$ and $Cu_2ZnSn(Se_{0.75}S_{0.25})_4$ by admittance and photoluminescence spectroscopy

E. Kask*, M. Grossberg, R. Josepson, P. Salu, K. Timmo, J. Krustok

Tallinn University of Technology, Department of Material Science, Ehitajate tee 5, 19086 Tallinn, Estonia

ARTICLE INFO

Available online 15 March 2013

Keywords:
$Cu_2ZnSnSe_4$
$Cu_2ZnSn(Se_{0.75}S_{0.25})_4$
Admittance spectroscopy
Photoluminescence spectroscopy
Defects

ABSTRACT

To achieve higher record efficiencies for solar cells containing $Cu_2ZnSnSe_4$ (CZTSe), Cu_2ZnSnS_4 (CZTS) or their solid solution $Cu_2ZnSn(Se_xS_{1-x})_4$ (CZTSSe) as an absorber, it is necessary to obtain more knowledge about defect structure of these materials. In this work, admittance spectroscopy (AS) and low temperature photoluminescence spectroscopy (PL) were used for defect studies. Admittance spectroscopy in the frequency range from 20 Hz to 10 MHz was used for studies of CZTSe/CdS and CZTSSe/CdS monograin layer heterojunctions. The measurement temperature varied from 140 K to 245 K. Two defect states (labelled E_{A1} and E_{A2}) were found in $Cu_2ZnSnSe_4$ and $Cu_2ZnSn(Se_{0.75}S_{0.25})_4$. In different CZTSe/CdS heterojunctions the E_{A2} state was present at 74 meV, but the second E_{A1} defect state changed from 87 meV to 100 meV during time and had varying properties. In $Cu_2ZnSn(Se_{0.75}S_{0.25})_4$ the E_{A2} state was found at 25 meV. The E_{A1} state at 154 meV showed the same properties as the two defect levels in CZTSe. In both cases the E_{A2} defect state was attributed to an acceptor defect and the E_{A1} state with changing properties to interface states. The detected PL bands were at 0.946 eV in CZTSe and at 1.028 eV in $Cu_2ZnSn(Se_{0.75}S_{0.25})_4$. Obtained by PL measurements, defect states at 69 meV in CZTSe and at 39 meV in $Cu_2ZnSn(Se_{0.75}S_{0.25})_4$ were attributed to the same acceptor defect that was found from the AS measurements.

1. Introduction

Quaternary compound $Cu_2ZnSnSe_4$ (CZTSe) is a promising non-toxic semiconductor material for absorber layer in solar cells [1]. CZTSe is an analogue of $CuInSe_2$ (CISe), where rare In is replaced with Zn and Sn. This CZTSe material has a direct band gap of about 1 eV [2,3] and high absorption coefficient ($>10^4\,cm^{-1}$) [4]. Bag et al. have studied CZTSe solar cells and conversion efficiency 10.1% was achieved [5]. $Cu_2ZnSn(S,Se)_4$ (CZTSSe) and Cu_2ZnSnS_4 (CZTS) devices with efficiencies of as high as 11.1% [6] and 8.4% [7], correspondingly, have been shown. Optimal band gap for solar energy conversion is achievable by choosing suitable S to Se ratio for CZTSSe solid solution. However, many physical properties of this compound are still unknown and CZTSe/CdS and CZTSSe/CdS heterojunctions have not been studied in detail. Furthermore, there is lack of information about the point defects in these absorber materials.

In fact, shallow defect levels with activation energies $E_A=27$ meV and $E_A=7$ meV have been found in CZTSe by photoluminescence (PL) as presented in Ref. [8]. We have previously studied CZTSe monograin powder by PL and found a low-temperature PL band at 0.946 eV that results from band-to-impurity (BI) recombination. The ionisation energy of the corresponding acceptor defect was found to be 69 meV [2].

The first-principles calculations have been made similar to CZTSe quaternary absorber CZTS by Chen et al. [9]. They found that the main acceptor defect in CZTS is Cu_{Zn}^- antisite defect that has quite deep level at $E_A=0.12$ eV. In our previous study the admittance spectroscopy (AS) on CZTS also showed deep acceptor level at $E_{A1}=0.12$ eV [10], that could be assigned to Cu_{Zn}^- acceptor defect.

* Corresponding author. Tel.: +372 620 3210.
E-mail address: erkki.kask@ttu.ee (E. Kask).

1369-8001/$ - see front matter © 2013 Elsevier Ltd. All rights reserved.
http://dx.doi.org/10.1016/j.mssp.2013.02.009

In addition, the second activation energy $E_{A2}=167$ meV was observed and attributed to the contribution of interface states. Similar results were attained by Fernandes et al. [11] who determined defect activation energies 44.7 meV and 112.7 meV. Gunawan et al. have studied CZTSSe absorber layer in solar cells by admittance spectroscopy and found E_A values in range 0.13–0.20 eV [12]. However, AS studies on CZTSe have not been reported so far. In the present paper AS and PL results of $Cu_2ZnSn(Se_{0.75}S_{0.25})_4$/CdS and $Cu_2ZnSnSe_4$/CdS monograin layer heterojunctions are presented.

2. Experimental

The CZTSe and CZTSSe monograin powders were synthesised from binary compounds. The chemical composition of monograin powder crystals was determined by energy dispersive X-ray analysis: Cu/(Zn+Sn)=0.88, Zn/Sn=1.0 for CZTSe and Cu/(Zn+Sn)=0.93, Zn/Sn=0.99 for $Cu_2ZnSn(Se_{0.75}S_{0.25})_4$. The single phase composition of CZTSe and CZTSSe was confirmed by Raman spectroscopy. Grains with diameters of 63–75 μm were selected by sieving and used for monolayer in the monograin layer CZTSe/CdS and CZTSSe/CdS heterojunctions. CdS buffer layer was chemically deposited onto powder crystals. Further details can be found in Ref. [13].

For temperature dependent AS measurements the CZTSe/CdS heterojunctions were mounted in the closed-cycle He cryostat (Janis) and the admittance spectra for CZTSe/CdS heterojunction were recorded by using a Wayne Kerr 6500B impedance analyser. Impedance Z and phase angle θ were both measured as functions of frequency and temperature. The used frequency range was from 20 Hz to 10 MHz and the temperature was varied from 140 K to 245 K with a step $\Delta T=5$ K. In order to maintain the linearity of the response signal, the AC voltage amplitude was kept as low as 10 mV. The measurements were carried out in the dark and with DC bias of 0 V.

In addition, the same monograin powders were studied by using photoluminescence (PL) spectroscopy in the temperature range of 10–140 K. For PL measurements, a He–Cd laser with the wavelength of 441 nm was used for PL excitation. The PL spectra were recorded by using a computer controlled SPM-2 monochromator ($f=40$ cm) together with an InGaAs detector and a DSP Lock-In amplifier SR 810.

The prepared CZTSe/CdS heterojunction was measured twice by AS. The first measurement after the preparation is referred to as the measurement of the fresh device in this paper. Then 2 months later the same CZTSe/CdS heterojunction (called aged device) was measured again. Between measurements no treatments on this heterojunction were performed.

3. Results and discussion

3.1. AS results

Admittance spectroscopy is a powerful tool for electrical characterisation of semiconductors. For defect studies, after each measurement the real and imaginary part of the impedance, Z' and $-Z''$ respectively, were calculated. The temperature dependence of Z' versus $-Z''$ graph of an aged CZTSe/CdS heterojunction is shown in Fig. 1. At every temperature curve consists of one arc and the corresponding equivalent circuit (see Fig. 1) was used for fitting the arcs. From the fittings the series resistance R_s values at each temperature were found. The R_s values were used to calculate the capacitance. Equivalent circuit, where serial resistor is followed by a resistor and a capacitor connected in parallel can be described by the following equation [14]:

$$Z = R_S + \frac{R_P}{1+(\omega R_P C)^2} - i\frac{R_P^2 C\omega}{1+(\omega R_P C)^2} \quad (1)$$

where ω, C, and R_P are angular frequency, capacitance, and parallel resistance, respectively. After rewriting (1), capacitance can be found by

$$C = \frac{-Z''}{\left[(Z'-R_S)^2+(-Z'')^2\right]\omega} \quad (2)$$

The capacitance C versus ω graphs are shown in Fig. 2.

The total capacitance consists of the free carrier capacitance across the width of the space charge region (SCR) and the additional capacitance contribution from charging and discharging of defect states at a location where the energy of electron (hole) states equals the electron (hole) quasi-Fermi level. Also, energetically continuous but locally discrete interface states contribute to total capacitance. The time constant for charging and recharging of defect states at energy equal to the quasi-Fermi level determines the inflection frequency i.e. step in the capacitance versus frequency spectrum. The additional capacitance occurs if the AC modulation allows the establishment of equilibrium between the occupation of the defect levels and the free carriers.

In case of an ideally discrete defect level, the dependence of the additional defect related capacitance C_d on the angular frequency ω is given by [15]:

$$C_d \propto \omega_0^2/(\omega_0^2-\omega^2) \quad (3)$$

where the inflection point at frequency ω_0 is related to the emission rate of the defect e_T. Therefore the temperature dependence of the inflection frequency ω_0 is presented by

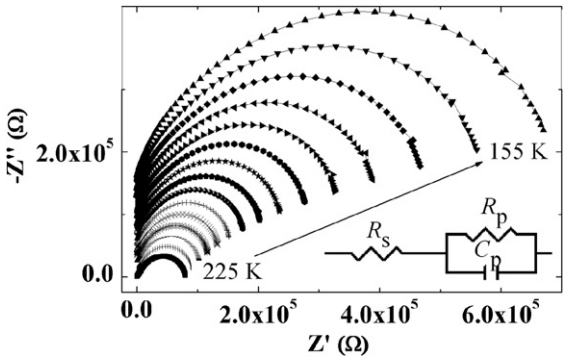

Fig. 1. Z' versus $-Z''$ graph of the aged CZTSe/CdS heterojunction. Equivalent circuit shown was used for fitting the arcs and finding R_s values at each temperature. The y-axis offset for arcs is set to 50%.

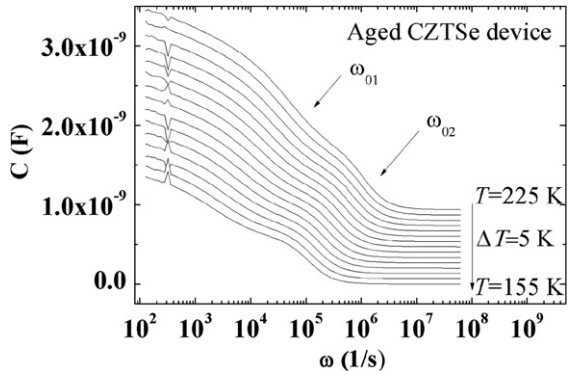

Fig. 2. The capacitance C versus ω graph of the aged CZTSe/CdS heterojunction. Steps, corresponding to inflection frequencies, are indicated by arrows. The y-axis offset for lines is set to 25%.

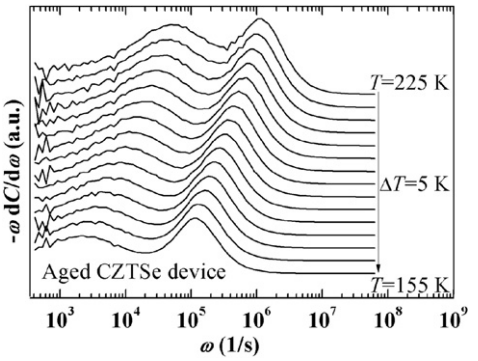

Fig. 3. The derivative $-\omega\,\mathrm{d}C/\mathrm{d}\omega$ versus ω graph of the aged CZTSe/CdS heterojunction depicts maxima which corresponding inflection frequencies ω_0 are used for the Arrhenius plot. The y-axis offset for lines is set to 50%.

[14–16]

$$\omega_0(T) = 2e_T(T) = 2N_{C,v}\upsilon_{th}\sigma_{n,p}\exp(-E_A/kT) = \\ = \xi_0 T^2 \exp(-E_A/kT) \quad (4)$$

where $N_{c,v}$ is the effective density of states in the conduction and valence band, v_{th} is the thermal velocity of charge carriers, $\sigma_{n,p}$ represents the capture cross-section for electrons and holes by the defect level. The emission prefactor ξ_0 covers all the temperature independent parameters. E_A is the activation energy of the defect level with respect to the corresponding band edge. The inflection frequency ω_0 corresponds to a maximum of $-\omega\,\mathrm{d}C/\mathrm{d}\omega$ versus ω graph.

After finding the natural logarithm of the Eq. (4) one can draw the Arrhenius plot of the inflection frequencies, $\ln(\omega_0/T^2)$ versus $10^3/T$. The linear fit is used for calculating activation energy of the defect level.

The $-\omega\,\mathrm{d}C/\mathrm{d}\omega$ versus ω graph of an aged CZTSe/CdS heterojunction is given in Fig. 3. This graph shows two maxima. Analogical dependences were found in CZTSSe/CdS heterojunction. The Arrhenius plots for all CZTSe measurements are shown in Fig. 4. All activation energies found by AS are in Table 1. The value of the activation energy at the higher frequency corresponding to E_{A2} state showed almost no changes during ageing time. At lower frequency (E_{A1} state) the fresh heterojunction shows quite different activation energy compared to the same but aged heterojunction: 87 meV and 100 meV, respectively.

The change (from 87 to 100 meV) in the second activation energy corresponding to E_{A1} state can probably be assigned to interface states. Possible change of interface properties with time could cause this change of activation energy. The stable activation energy at 74 meV is obviously related to some deep acceptor defect state. In CZTS the activation energy of 120 meV belonged to Cu_{Zn}^{-} acceptor defect [9,10]. Considering that the activation energy of a defect varies with the band-gap of different materials, i.e. for similar compounds $CuInSe_2$ and $CuInS_2$ [17,18], 74 meV of CZTSe could to be related to the same Cu_{Zn}^{-} acceptor defect, but this assumption needs some further studies. As in CZTSe the p–d hybridisation is smaller and the valence band is higher, then it is expected that the activation energy of the Cu_{Zn}^{-} defect decreases

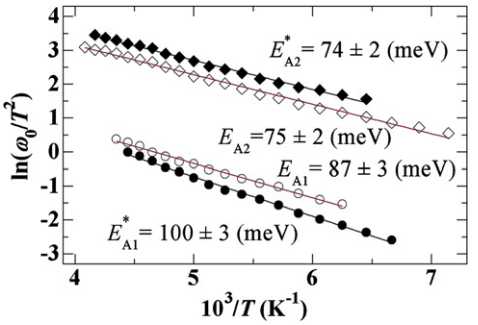

Fig. 4. The Arrhenius plot of the CZTSe/CdS heterojunction showing the activation energy values, where E_{A2} are for defect state and E_{A1} for interface states. White symbols and E_{A2} and E_{A1} correspond to the fresh device measurement, the black filled symbols and E^*_{A2} and E^*_{A1} show results for aged device. All dependencies were fitted with a linear function.

Table 1
Activation energies found by AS and PL of the measured heterojunctions. In brackets are results for aged device.

Material	AS results		PL results
	E_{A1} (meV)	E_{A2} (meV)	E_T (meV)
$Cu_2ZnSn(Se_{0.75}S_{0.25})_4$	154 ± 7	25 ± 5	39 ± 5
$Cu_2ZnSnSe_4$	87 ± 3 (100 ± 3)	75 ± 2 (74 ± 2)	69 ± 4

with increasing Se concentration in $Cu_2ZnSn(Se_xS_{1-x})_4$ [19]. As materials inspected are deficient in copper, V_{Cu}^{-} acceptors should also be present. Moreover, donor–acceptor defect complexes are also expected in this material. In CZTS and CZTSe the Cu_{Zn}^{-} antisite is deeper acceptor than V_{Cu}^{-} [9] and therefore can be detected by AS.

3.2. PL results

In Fig. 5(b) normalised PL spectra of the CZTSe and $Cu_2ZnSn(Se_{0.75}S_{0.25})_4$ monograins measured at $T = 10$ K are given. Both PL spectra show an asymmetric PL band at 0.946 eV for CZTSe and at 1.028 eV for $Cu_2ZnSn(Se_{0.75}S_{0.25})_4$. The asymmetric shape of the PL bands is an indication of the

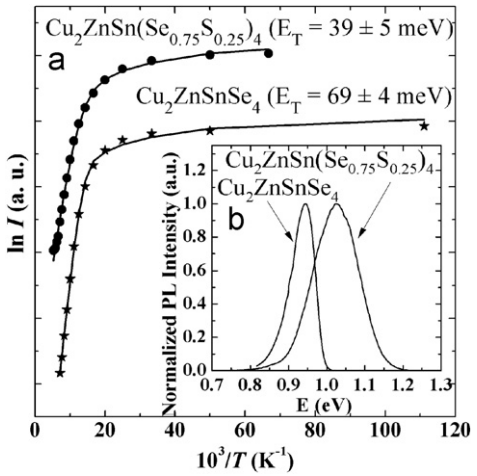

Fig. 5. The normalised PL spectra at 10 K (b) [21] and the Arrhenius plot derived from the temperature dependencies of these PL spectra (a).

presence of spatial potential fluctuations in the material [20] that are caused by high concentration of randomly distributed charged defects. The potential fluctuations are often found in multinary compounds where the native defect concentrations are usually very high [2,3,21]. These potential fluctuations lead to a local perturbation of the electronic band structure, thus broadening the defect level distribution and forming band tails [20]. Radiative recombination in the material containing spatial potential fluctuations can mainly arise from three different recombination channels. First, in band-to-band (BB) recombination a free electron recombines with a free hole. Second, in band-to-tail (BT) recombination a free electron recombines with a hole that is localised in the potential wells of the valence band tail. Third, in band-to-impurity (BI) recombination a free electron recombines with a hole that is localised on a deep acceptor level that is deep enough not to overlap with the valence band tail.

Temperature dependent and excitation power dependent measurements of the PL spectra indicate that the PL bands result from the BI—recombination. A strong blue-shift with a magnitude of 17 meV per decade for CZTSe and 11 meV per decade for $Cu_2ZnSn(Se_{0.75}S_{0.25})_4$ with increasing excitation power was detected. The Arrhenius plots derived from the temperature dependencies of the PL spectra [21] together with the fitting curves are presented in Fig. 5(a). For the fitting the temperature dependence of the integral intensity formula was used [22]

$$I(T) = I_0 / \left(1 + c_1 T^{3/2} + c_2 T^{3/2} \exp(-E_T/kT)\right) \quad (5)$$

where E_T is the activation energy. ln$I$ versus $10^3/T$ is used for the Arrhenius plot that shows linear behaviour at high temperatures which is characteristic for BI-recombination. The obtained defect ionisation energies, E_T can be found in Table 1.

By summarizing AS and PL results, defect ionisation energies found by PL are attributed to the same acceptor defects that were found from AS measurements, respectively. In CZTSSe the activation energy of the E_{A2} state seems not to be related to the same defect as in CZTSe or CZTS, but this behaviour needs further studies.

4. Conclusions

Admittance and photoluminescence spectroscopy were used for investigating defect levels in CZTSe/CdS and $Cu_2ZnSn(Se_{0.75}S_{0.25})_4$/CdS heterojunctions. Two defect states were observed in both materials by AS. The unstable defect state showed activation energies from 87 meV to 100 meV in CZTSe. This defect state was attributed to the interface states because possible change of interface properties with time could cause change of activation energy. The stable deep defect state in CZTSe was found to be at 74 meV and this could belong to Cu_{Zn}^{-} acceptor defect, but this assumption needs further studies. In CZTSSe activation energies 154 meV and 25 meV were found. In addition, these materials were studied by photoluminescence spectroscopy. An asymmetric PL band at 0.946 eV in CZTSe and at 1.028 eV in $Cu_2ZnSn(Se_{0.75}S_{0.25})_4$ were detected at 10 K. The obtained E_{A2} defect states at 69 meV for CZTSe and at 39 meV for $Cu_2ZnSn(Se_{0.75}S_{0.25})_4$ were attributed to the same acceptor defects that were found from AS measurements.

Acknowledgements

This work was supported by the Estonian Science Foundation Grants G-8282 and ETF 9369, by the Target Financing by HTM (Estonia) (No. SF0140099s08), Estonian Centre of Excellence in Research, Project TK117T, and by Materials Technology program. The support of the World Federation of Scientists National Scholarship Programme is gratefully acknowledged. The authors thank also the CZTSSe-team at the TUT.

References

[1] D.B. Mitzi, O. Gunawan, T.K. Todorov, K. Wang, S. Guha, Solar Energy Materials and Solar Cells 95 (2011) 1421.
[2] M. Grossberg, J. Krustok, K. Timmo, M. Altosaar, Thin Solid Films 517 (2009) 2489.
[3] J. Krustok, R. Josepson, T. Raadik, M. Danilson, Physica B 405 (2010) 3186.
[4] K. Ito, T. Nakazawa, Japanese Journal of Applied Physics 27 (1988) 2094.
[5] S. Bag, O. Gunawan, T. Gokmen, Y. Zhu, T.K. Todorov, D.B. Mitzi, Energy and Environmental Science 5 (2012) 7060.
[6] T.K. Todorov, J. Tang, S. Bag, O. Gunawan, T. Gokmen, Y. Zhu, D.B. Mitzi, Advanced Energy Materials 3 (2013) 34.
[7] B. Shin, O. Gunawan, Y. Zhu, N.A. Bojarczuk, S.J. Chey, S. Guha, Progress in Photovoltaics: Research and Applications 21 (2013) 72.
[8] F. Luckert, D.I. Hamilton, M.V. Yakushev, N.S. Beattie, G. Zoppi, M. Moynihan, I. Forbes, A.V. Karotki, A.V. Mudryi, M. Grossberg, J. Krustok, R.W. Martin, Applied Physics Letters 99 (2011) 062104.
[9] S. Chen, J.-H. Yang, X.G. Gong, A. Walsh, S.-H. Wei, Physical Review B 81 (2010) 245204.
[10] E. Kask, T. Raadik, M. Grossberg, R. Josepson, J. Krustok, Energy Procedia 10 (2011) 261.
[11] P.A. Fernandes, A.F. Sartori, P.M.P. Salomé, J. Malaquias, A.F. da Cunha, et al., Applied Physics Letters 100 (2012) 233504.
[12] O. Gunawan, T. Gokmen, C.W. Warren, J.D. Cohen, T.K. Todorov, et al., Applied Physics Letters 100 (2012) 253905.
[13] M. Altosaar, J. Raudoja, K. Timmo, M. Danilson, M. Grossberg, J. Krustok, E. Mellikov, Physica Status Solidi A 205 (2008) 167.
[14] H. Bayhan, A.S. Kavasoğlu, Turkish Journal of Physics 27 (2003) 529.
[15] R. Herberholz, M. Igalson, H.W. Schock, Journal of Applied Physics 83 (1998) 318.

[16] A. Jasenek, U. Rau, V. Nadenau, H.W. Schock, Journal of Applied Physics 87 (1) (2000) 594.
[17] S. Zott, K. Leo, M. Ruckh, H.W. Schock, Applied Physics Letters 68 (1996) 1144.
[18] J.H. Schön, E. Bucher, Physica Status Solidi A 171 (1999) 511.
[19] S. Chen, A. Walsh, J.-H. Yang, X.G. Gong, L. Sun, P.-X. Yang, J.-H. Chu, S.-H. Wei, Physical Review B 83 (2011) 125201.
[20] A.P. Levanyuk, V.V. Osipov, Soviet Physics Uspekhi 24 (1981) 187.
[21] M. Grossberg, J. Krustok, J. Raudoja, K. Timmo, M. Altosaar, T. Raadik, Thin Solid Films 519 (2011) 7403.
[22] J. Krustok, H. Collan, K. Hjelt, Journal of Applied Physics 81 (3) (1997) 1442.